Thermodynamic properties of a harmonically trapped, two-dimensional charged quantum gas in a magnetic field

2008 J. Phys. A: Math. Theor. 41 135305

(http://iopscience.iop.org/1751-8121/41/13/135305)

IOP PUBLISHING JOURNAL OF PHYSICS A: MATHEMATICAL AND THEORETICAL

J. Phys. A: Math. Theor. **41** (2008) 135305 (16pp) doi:10.1088/1751-8113/41/13/135305

Thermodynamic properties of a harmonically trapped, two-dimensional charged quantum gas in a magnetic field

Patrick Shea and Brandon P van Zyl

Department of Physics, St. Francis Xavier University, Antigonish, Nova Scotia, Canada

Received 2 October 2007, in final form 18 February 2008
Published 14 March 2008
Online at stacks.iop.org/JPhysA/41/135305

Abstract

We present exact analytical results for the thermodyanmic properties of a two-dimensional (2D), harmonically trapped charged quantum gas in a magnetic field. While our results are applicable to both Fermi and Bose gases, we focus our attention on trapped fermions owing to their relevant application in the density-functional theory of inhomogeneous Fermi systems. In particular, we test the Thomas–Fermi (or continuum) approximation (TFA) for the functional relation $\tau[\rho]$ using the exact $\rho(r)$ and show that it reproduces the local and global properties of the exact kinetic energy density $\tau(r)$ surprisingly well. However, when we compare our exact results for various thermodynamic quantities with the TFA, we find that it misses several important features. These deviations are shown to be entirely due to the quantum mechanical properties of the system, which are not accounted for in the continuum approximation.

PACS numbers: 03.75.Ss, 05.30.Fk

1. Introduction

In a very recent paper, we have provided an exact, analytical expression for the finite-temperature first-order density matrix (FDM) of a charged, 2D, harmonically trapped quantum gas in the presence of a constant magnetic field [1, 2]. While the primary goal of that work was to obtain an exact closed form expression for the FDM, it was noted that a very useful application would be a detailed analytical investigation of the thermodynamic properties of the 2D trapped charged quantum gas, as derived from the FDM. The motivation for such a study is founded on some of the interesting properties of ultra-cold, 2D harmonically trapped Fermi gases, uncovered by one of us and Brack [3]. Specifically, in [3], it was shown analytically that for the special case of 2D, the Thomas–Fermi (TF) density-functional theory (DFT) at zero magnetic field reproduces the exact spatial variations found for the particle and kinetic energy densities, extremely well, except near the classical turning point.

More remarkable, however, was the discovery that the simple TF DFT—*without gradient corrections*—yields the *exact* quantum mechanical energy of the system for any number of filled shells, in spite of the fact that the TF theory cannot be variationally exact. The fact that the simple TF DFT in 2D is in agreement with the full quantum mechanical calculation is thus highly non-trivial, since TF DFT is theoretically exact only in the local-density approximation (LDA). This finding has direct relevance in DFT, where the TFA is widely used to establish explicit expressions for the various energy density functionals of inhomogeneous Fermi systems.

With applications to DFT in mind, it is perhaps then natural to ask just how well the TFA holds when one also includes the presence of an external magnetic field perpendicular to the inhomogeneous 2D system (e.g., quantum dots in a constant magnetic field). While Brack and van Zyl have already provided the answer to this question for the case of zero magnetic field, to our knowledge, no analogous *analytical* investigation including the presence of an external magnetic field has yet been performed. In view of the fact that semiclassical approaches (such as the TF DFT) are a very valuable tool for providing simple insight into otherwise difficult many-body systems, our motivation for extending the results of [3] to include an external magnetic field is therefore not purely academic. Indeed, one need only look as far as the relatively recent works of Schneider and Wallis [4] and Toms [5], for additional impetus for our proposed extension. Specifically, these papers have investigated the thermodynamic properties of an ideal, harmonically trapped Fermi gas using numerical [4] and analytical [5] approaches, with the key finding being that there are step-like features in thermodynamic quantities of the system beyond what is obtained in the continuum approximation.

An analytical investigation of the step-like features found for the thermodynamic quantities (e.g., chemical potential and specific heat) was performed by Toms [5], in which the steps were understood as a consequence of the de Haas-van Alphen part of the thermodynamic potential. This analysis, however, was limited to the case of zero magnetic field, thereby rendering it difficult to obtain any additional insight into how these purely quantum mechanical features are altered when an external magnetic field is imposed. In view of Toms' interpretation of the step-like features in terms of the de Haas-van Alphen-type effect, it seems a logical progression to further investigate the system discussed above when an external magnetic field is present. The purpose of the present work then, is to give a detailed, analytical study of the thermodynamic properties of a 2D harmonically trapped charged quantum gas in a constant external magnetic field of arbitrary strength and at finite temperature. Owing to the fact that our analysis includes an external magnetic field *a priori*, the results we present here are more general than those found in [3–5], the latter results being essentially special cases of the current investigation.

The rest of our paper is organized as follows. In the next section, we provide a detailed derivation of the exact kinetic energy density of a 2D harmonically trapped quantum gas at finite temperature. This expression is then compared with the widely used TFA for the kinetic energy density, where we focus on how well the TFA holds for both the local (i.e., spatial) and global (i.e., integrated) properties of the system. Following this, we examine the step-like features found for the integrated kinetic energy (which are most prominent at zero temperature) with a view to obtaining a simple physical explanation for the origin of these structures. Subsequent to this, we then examine the chemical potential at both zero and finite magnetic fields, and again study the origin of the step-like features, in addition to comparing the exact expressions with their TF counterparts. We also demonstrate analytically how the exact expressions for various thermodynamic quantities approach the TFA in the appropriate limits, and provide simplified expressions for the exact results in the limits of strong and weak magnetic fields.

2. Kinetic energy

The system under consideration is an ideal gas of harmonically trapped fermions (or spinless charged bosons) in two dimensions, with a potential $V(\vec{r}) = \frac{1}{2}m\omega_o r^2$. Also included is a magnetic field of constant magnitude in the perpendicular direction, with vector potential, in the symmetric gauge, given by $\vec{A} = \left(-\frac{1}{2}By, \frac{1}{2}Bx, 0\right)$. The Hamiltonian is thus given by

$$H_r = -\frac{\hbar^2}{2m}\nabla^2 + i\hbar\omega_c\left(x\frac{\partial}{\partial y} - y\frac{\partial}{\partial x}\right) + \frac{1}{2}m\omega_{\text{eff}}r^2, \tag{1}$$

where $\omega_c = \frac{eB}{2mc}$ is the Larmor frequency, and $\omega_{\text{eff}} = \sqrt{\omega_o^2 + \omega_c^2}$ is the effective frequency. In what follows, we have scaled all lengths by $\sqrt{\frac{\hbar}{m\omega_{\text{eff}}}}$, and all energies by $\hbar\omega_{\text{eff}}$, with the magnetic field strength being encoded in the dimensionless quantity $\omega = \omega_c/\omega_{\text{eff}}$. We will also assume, in all calculations, a spin degeneracy factor of 2. In the case of spinless charged bosons, the spin degeneracy factor of 2 should be omitted. We have neglected the coupling between the spin of the fermions and the magnetic field in equation (1), since it just adds a constant term to the Hamiltonian if, for example, the spins are taken to be anti-parallel to the field. We also wish to point out that equation (1) has the same form for a cranked harmonic oscillator, whose energy eigenvalues are identical to those of a deformed 2D harmonic oscillator [8, 11]. This fact has previously been used by Habeeb [12] to derive the Bloch density matrix for the system.

2.1. Exact kinetic energy density

To calculate the exact kinetic energy density, we will start from the first-order density matrix for the system, which has been reported earlier [1, 2], and is given by the following expression:

$$\rho(\vec{r}, \vec{r}_0) = \frac{2}{\pi}\sum_{l=0}^{\infty}\sum_{m=0}^{\infty}\sum_{n=0}^{\infty} L_l^{m+n}(2\mathcal{A})\frac{\mathcal{B}^m}{m!}\frac{\mathcal{B}^{*n}}{n!}\,\mathrm{e}^{-\mathcal{A}} f_{lmn}(\mu, T), \tag{2}$$

where

$$\mathcal{A} = \tfrac{1}{2}\left(x^2 + y^2 + x_0^2 + y_0^2\right), \qquad \mathcal{B} = xx_0 + yy_0 + i(x_0y - y_0x), \tag{3}$$

and $L_\lambda^\nu(x)$ is an associated Laguerre polynomial [6]. The function $f_{lmn}(\mu, T)$ is the Fermi function:

$$f_{lmn}(\mu, T) = \frac{1}{\exp\left(\frac{\epsilon_{lmn} - \mu}{T}\right) + 1} = \frac{1}{\exp\left(\frac{1+2l+m+n+\omega(n-m)-\mu}{T}\right) + 1}, \tag{4}$$

where T denotes the dimensionless quantity $k_BT/\hbar\omega_{\text{eff}}$. Unless otherwise noted, we will focus on the limit $T \to 0$, since it is in this regime where the quantum effects that we wish to investigate are most prominent. In this limit the Fermi function approaches the unit step function, $f_{lmn} \to \Theta(\epsilon_f - \epsilon_{lmn})$, where ϵ_f is the Fermi energy, and has the effect of truncating the infinite sums at finite values of l, m and n.

The exact kinetic energy density is thus obtained by inserting equation (2) into the well-known expression

$$\tau(\vec{r}) = [H_r - V(\vec{r})]\rho(\vec{r}, \vec{r}_0)|_{\vec{r}=\vec{r}_0} \tag{5}$$

where H_r denotes the Hamiltonian with respect to the variable $\vec{r} = (x, y)$. The resulting expression from this calculation is given by

$$\tau(\vec{r}) = \sum_{l,m,n} f_{l,m,n}(\mu, T)\Bigg[(m+n+1)L_l^{m+n+1}(2r^2) + \left(l + \omega(n-m) + \frac{1}{2}r^2(\omega^2-1) - 2mn/r^2\right)L_l^{m+n}(2r^2)\Bigg]\frac{r^{2(m+n)}}{m!n!}\,\mathrm{e}^{-r^2}, \tag{6}$$

where the Laguerre differential equation, and recursion relation between the Laguerre polynomials have been used to simplify [6]. While equation (6) is exact, there is an alternative approach based on the explicit single-particle wavefunctions, which results in a much simpler expression for the kinetic energy density, and is more convenient for some of the calculations presented below.

By using the creation and annihilation operators for a 2D harmonic oscillator in a magnetic field, one can show that the single-particle eigenfunctions are given by

$$\psi_{MN}(\vec{r}) = \sqrt{\frac{M!}{\pi N!}}r^{N-M}\,\mathrm{e}^{\mathrm{i}(N-M)\theta}L_M^{N-M}(r^2)\,\mathrm{e}^{-r^2/2}, \tag{7}$$

with energy eigenvalues

$$\epsilon_{MN} = 1 + M + N + \omega(N-M), \qquad M, N = 0, 1, 2, \ldots. \tag{8}$$

The interpretation of M and N is as follows. In the limit that the strength of the harmonic oscillator trap goes to zero, N will be the index of the Landau levels. In the limit that the strength of the magnetic field goes to zero, $M + N$ will be the index of the harmonic oscillator shells (denoted by s in this paper). The eigenvalue of the z-component of the angular momentum is $N - M$. Now, setting $\vec{r}_0 = \vec{r}$ in equation (2), we obtain the particle density:

$$\rho(\vec{r}) = \frac{2}{\pi}\sum_{l=0}^{\infty}\sum_{m=0}^{\infty}\sum_{n=0}^{\infty}L_l^{m+n}(2r^2)\frac{r^{2(m+n)}}{m!n!}\,\mathrm{e}^{-r^2}f_{lmn}(\mu, T). \tag{9}$$

Making use of the the above eigenfunctions, the particle density may also be written as

$$\rho(\vec{r}) = \sum_{M=0}^{\infty}\sum_{N=0}^{\infty}|\psi_{MN}(\vec{r})|^2 f_{MN}(\mu, T), \tag{10}$$

where the Fermi function $f_{MN}(\mu, T)$ is equation (4) with ϵ_{lmn} replaced by the energy eigenvalues ϵ_{MN}, as given in equation (8). With a view to comparing equations (9) and (10), we will redefine the summation indices in equation (9) such that the Fermi function f_{lmn} has the same form as f_{MN}. This requires that $l + m = M$, and $l + n = N$ (see equations (4) and (8)). Making this substitution gives

$$\rho(r) = \frac{2}{\pi}\sum_{M=0}^{\infty}\sum_{N=0}^{\infty}\sum_{l=0}^{M,N}L_l^{M+N-2l}(2r^2)\frac{r^{2(M+N-2l)}}{(M-l)!(N-l)!}\,\mathrm{e}^{-r^2}f_{MN}(\mu, T), \tag{11}$$

where the limit in the l-sum is the lower of either M or N (this ensures that l, m, and n are always $\geqslant 0$, as required). The l-sum may be evaluated by making use of the summation relation [6]

$$\sum_{k=0}^{n}L_{n-k}^{\alpha+2k}(x+y)\frac{(xy)^k}{k!(k+\alpha)!} = L_n^{\alpha}(x)L_n^{\alpha}(y)\frac{n!}{(n+\alpha)!}, \tag{12}$$

and the relation

$$\sqrt{\frac{M!}{N!}}r^{N-M}L_M^{N-M}(r^2) = \sqrt{\frac{N!}{M!}}r^{M-N}L_N^{M-N}(r^2), \tag{13}$$

from which it can be shown that

$$\sum_{l=0}^{M,N} L_l^{M+N-2l}(2r^2)\frac{r^{2(M+N-2l)}}{(M-l)!(N-l)!}\,\mathrm{e}^{-r^2} = \frac{M!}{N!}\left[L_M^{N-M}(r^2)\right]^2 r^{2(N-M)}\,\mathrm{e}^{-r^2} = |\psi_{MN}(\vec{r})|^2, \tag{14}$$

as expected if equations (10) and (11) are equal.

We are now in a position to calculate a much simplified form for the kinetic energy density. We note that equation (5) may be written as

$$\tau(\vec{r}) = \sum_{\text{all } i}[H_r - V(\vec{r})]\psi_i^*(\vec{r}_0)\psi_i(\vec{r})\,f_i(\mu, T)|_{r_0=r}, \tag{15}$$

and after inserting the eigenfunctions, equation (7), into (15), we obtain

$$\tau(\vec{r}) = \frac{2}{\pi}\sum_{M=0}^{\infty}\sum_{N=0}^{\infty}\frac{M!}{N!}\left(\epsilon_{MN} + \frac{1}{2}(\omega^2-1)r^2\right)\left[L_M^{N-M}(r^2)\right]^2 r^{2(N-M)}\,\mathrm{e}^{-r^2} f_{MN}(\mu, T). \tag{16}$$

Inserting the summation relation, equation (14), into (16) gives

$$\tau(\vec{r}) = \frac{2}{\pi}\sum_{M=0}^{\infty}\sum_{N=0}^{\infty}\sum_{l=0}^{M,N}\left(\epsilon_{MN} + \frac{1}{2}(\omega^2-1)r^2\right)L_l^{M+N-2l}(2r^2) \times \frac{r^{2(M+N-2l)}}{(M-l)!(N-l)!}\,\mathrm{e}^{-r^2} f_{MN}(\mu, T), \tag{17}$$

which, upon reverting to the original indices l, m, n, reads

$$\tau(\vec{r}) = \frac{2}{\pi}\sum_{l=0}^{\infty}\sum_{m=0}^{\infty}\sum_{n=0}^{\infty}\left(\epsilon_{lmn} + \frac{1}{2}(\omega^2-1)r^2\right)L_l^{m+n}(2r^2)\frac{r^{2(m+n)}}{m!n!}\,\mathrm{e}^{-r^2} f_{lmn}(\mu, T). \tag{18}$$

Note that equation (18) is analytically much simpler than equation (6). Moreover, upon comparison with equation (16) we note that equation (18) contains only single $L_\lambda^\nu(2r^2)$ terms, whereas equation (16) contains $\left[L_\lambda^\nu(r^2)\right]^2$ terms, in addition to inverse powers of r. From a numerical point of view, such singular terms (i.e., as $r \to 0$) are not desirable, although they do conspire to yield a finite result for $\tau(0)$ provided enough terms in the series are retained.

Equation (18) is to be viewed as a generalization of the 2D result presented in [2][1], where only the case of zero-magnetic field was studied. It is also worth mentioning again that equation (18) is also directly applicable to a charged, 2D trapped spinless Bose gas (see, e.g., [7]) provided the '+1' in the denominator of equation (4) is changed to a '−1' and the spin degeneracy factor of 2 is omitted. To our knowledge, the above explicit analytical expressions for $\tau(\vec{r})$ at finite temperature have not appeared in the literature.

2.2. *Thomas–Fermi approximation*

2.2.1. Local properties. Having obtained an exact expression for $\tau(\vec{r})$, we now proceed to first compare its local (i.e., spatial) properties with the TFA (or LDA) of the kinetic energy density. This is in the spirit of the analytical study presented in [3] in which the same comparison was made, but only for the case of zero magnetic field.

The TFA to the kinetic energy density can be obtained by making use of the systematic Wigner–Kirkwood (WK) semiclassical expansion [8]. In this approach, the FDM is written as an (asymptotic) series in powers of $\hbar$ with the term to zeroth order in $\hbar$ yielding the TFA.

[1] Simplified analytical expressions of the results presented in [1] can be found in [2].

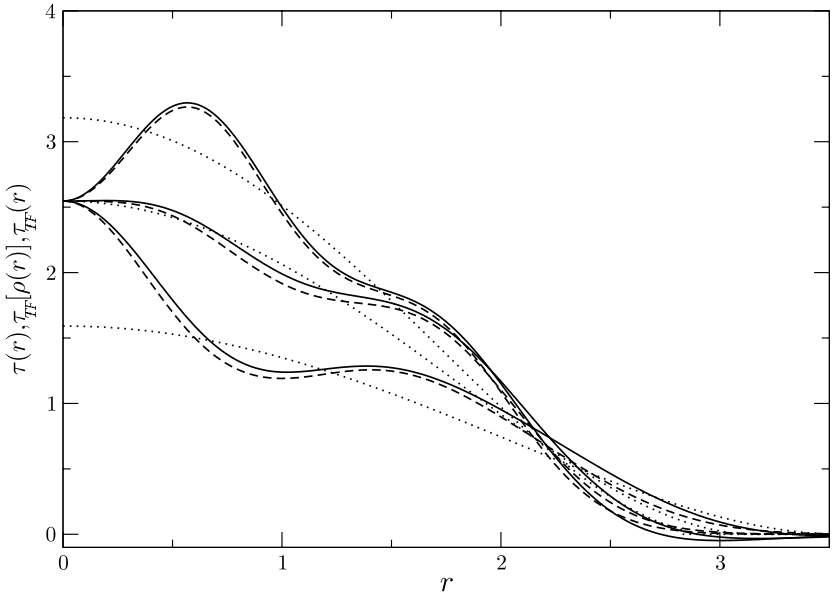

Figure 1. The $T = 0$ kinetic energy density for $\mathcal{N} = 20$ particles. The three sets of curves are for, from top to bottom, $\frac{\omega_c}{\omega_o} = 0, 0.5, 1$, corresponding to $\omega = 0, \frac{1}{\sqrt{5}}, \frac{1}{\sqrt{2}}$. The solid lines are the exact densities, the dashed lines are the Thomas–Fermi functional [equation (19]with exact density inserted, and the dotted lines are the pure Thomas–Fermi densities (i.e., equation (19) with (20) inserted). This same convention is used for all figures.

If terms of higher order in $\hbar$ are retained, the so-called gradient corrections associated with the inhomogeniety of the system are obtained. The details of this approach can be found in [8], and as they are not immediately pertinent to the present work, we simply provide the final expression for the TFA of the kinetic energy density, leaving the details of the calculation to a future work (see also [7, 9]):

$$\tau_{\mathrm{TF}}[\rho(\vec{r})] = \frac{\pi}{2}[\rho(\vec{r})]^2. \tag{19}$$

Interestingly, the TF kinetic energy density above has the same functional form as that of the free 2D system in the absence of a magnetic field, but here, the spatial magnetic field dependence is encoded in the density ρ. Note that this is not the case for 3D, whereby the form of the TFA of the kinetic energy functional explicitly depends on the strength of the magnetic field. As mentioned above, there are gradient corrections to equation (19), but as our present motivation is to investigate how well the exact results compare with the LDA (i.e., analogous to the study in [3]), we will not consider them here. The TFA to the particle density obtained from the WK semiclassical expansion technique is given by (in our scaled units)

$$\rho_{\mathrm{TF}}(\vec{r}) = \frac{1}{\pi}\left[\epsilon_f^{\mathrm{TF}} - \frac{1}{2}(1-\omega^2)r^2\right]\Theta\left[\epsilon_f^{\mathrm{TF}} - \frac{1}{2}(1-\omega^2)r^2\right], \tag{20}$$

where ϵ_f^{TF} is the TFA to the Fermi energy.

Figure 1 shows the $T = 0$ spatial dependence of the kinetic energy density for $\mathcal{N} = 20$ particles. Included in this plot are the exact density, the TF functional, equation (19) with the exact particle density, equation (9) inserted (which we will refer to as TF functional), and the smooth TF density, i.e. equation (19) with the TF particle density, equation (20), inserted (which we will refer to as pure TF), shown for several magnetic field strengths. As seen from the figure, the TF functional reproduces even the local spatial oscillations in the

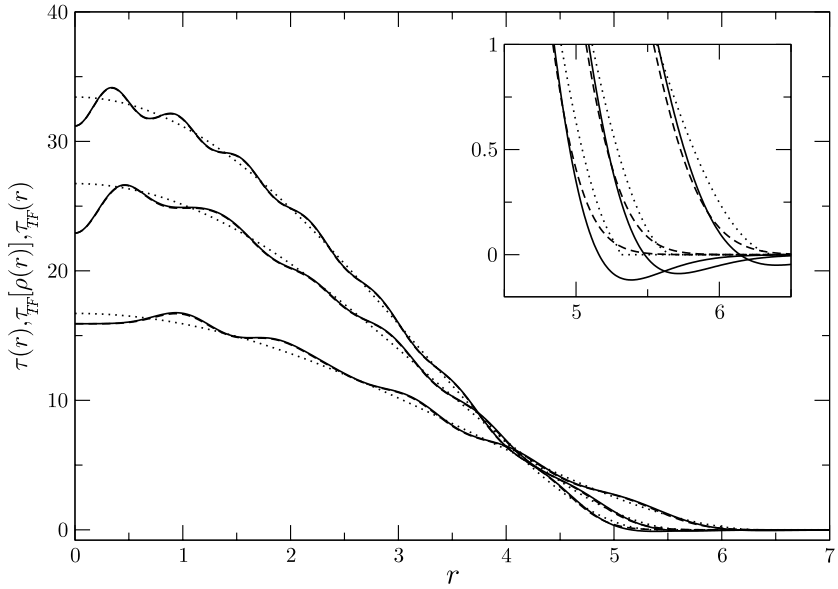

Figure 2. Same as figure 1, but for $\mathcal{N} = 210$ particles. The inset shows a close-up around the tail region.

density remarkably well. The pure TF density is a smooth curve which the exact density $\tau(\vec{r})$ oscillates around. This has already been observed in [3] for the case of zero magnetic field, but it is now evident from figure 1 that a similar behaviour also holds when a constant external magnetic field is introduced.

In addition to the TF functional being surprisingly accurate at low numbers of particles, it was also shown in [10] that in the limit as $\mathcal{N} \to \infty$, the TF functional, $\tau_{\mathrm{TF}}[\rho(\vec{r})]$, approaches the exact kinetic energy density (in the absence of a magnetic field). To investigate whether this result holds in the presence of a magnetic field, figure 2 shows the kinetic energy densities for a higher number of particles, $\mathcal{N} = 210$. Even at this relatively low number of particles the kinetic energy densities are nearly indistinguishable. The inset shows a close-up near the tail region, where the deviations between the densities are most noticeable. The numerical evidence we have presented here strongly suggests that the result of [10] also holds in the presence of a magnetic field. Note that the remarkable agreement between the exact and TF functional is quite unexpected, particularly because of the fact that the TFA to the kinetic energy density has no explicit magnetic field dependence and can be obtained by simply using the zero-field expressions for the densities. This result does not appear to have been noticed before.

Referring again to figures 1 and 2, it is also interesting to note that the exact density and TF functional appear to be in exact agreement at $r = 0$ in both figures. It is straightforward to show analytically that this is in fact the case. Starting from equation (18), the only non-zero terms at $r = 0$ will be for $m = n = 0$. We therefore obtain the exact density as (at $T = 0$)

$$\tau(0) = \frac{2}{\pi}\sum_{l=0}^{\infty} f_{l00}(\mu, T=0)\epsilon_{l00}L_l^0(0) = \frac{2}{\pi}\sum_{l=0}^{\lfloor\frac{\epsilon_f-1}{2}\rfloor}(2l+1)$$
$$= \frac{2}{\pi}\left(\left\lfloor\frac{\epsilon_f-1}{2}\right\rfloor+1\right)^2, \tag{21}$$

where $\lfloor x \rfloor$ denotes the floor function; i.e., the largest integer less than or equal to x. The exact particle density at $r = 0$ is (again with $m = n = 0$)

$$\rho(0) = \frac{2}{\pi} \sum_{l=0}^{\lfloor \frac{\epsilon_f - 1}{2} \rfloor} L_l^0(0) = \frac{2}{\pi} \left(\left\lfloor \frac{\epsilon_f - 1}{2} \right\rfloor + 1 \right), \tag{22}$$

so that the TF kinetic energy density is

$$\tau_{\mathrm{TF}}(0) = \frac{\pi}{2} \rho(0)^2 = \frac{2}{\pi} \left(\left\lfloor \frac{\epsilon_f - 1}{2} \right\rfloor + 1 \right)^2. \tag{23}$$

Thus the exact and TF functional kinetic energy densities at $r = 0$ agree for any number of particles and magnetic field strength.

2.2.2. Global properties. To further test the validity of the TFA for this system, we now investigate the total kinetic energy, obtained by integrating the kinetic energy density over all space. For this calculation it will be simpler to use the form for the kinetic energy density given in equation (16). Integrating over all space, one obtains for the exact total kinetic energy [6]:

$$E_{\mathrm{kin}} = \sum_{N=0}^{\lfloor \frac{\epsilon_f - 1}{1+\omega} \rfloor} \sum_{M=0}^{\lfloor \frac{\epsilon_f - 1 - (\omega+1)N}{1-\omega} \rfloor} \left((\omega^2 + 1) + (\omega - 1)^2 M + (\omega + 1)^2 N \right) \tag{24}$$

$$= \sum_{N=0}^{\lfloor \frac{\epsilon_f - 1}{1+\omega} \rfloor} \left(\left\lfloor \frac{\epsilon_f - 1 - (\omega+1)N}{1-\omega} \right\rfloor + 1 \right) \times \left((\omega^2 + 1) + (\omega + 1)^2 N + \frac{(\omega - 1)^2}{2} \left\lfloor \frac{\epsilon_f - 1 - (\omega+1)N}{1-\omega} \right\rfloor \right). \tag{25}$$

Inserting equation (2) into the TF functional and integrating yields [6]

$$E_{\mathrm{kin}}^{\mathrm{TF}} = \sum_{l,m,n} \sum_{l',m',n'} \frac{\Theta(\epsilon_f - \epsilon_{lmn}) \Theta(\epsilon_f - \epsilon_{l'm'n'})}{m!n!m'!n'!2^{m+n+m'+n'}} \times (-1)^{l+l'} (m + n + m' + n')! \binom{l + m + n}{l'} \binom{l' + m' + n'}{l}. \tag{26}$$

While equation (26) may look somewhat cumbersome, it is nevertheless a simpler numerical procedure than a direct numerical integration of equation (19) with the exact density inserted as input.

As mentioned above, it was found in [3] that in the absence of a magnetic field, the TF functional (with the exact density inserted) integrates to the exact total kinetic energy. To test this result in the presence of a magnetic field, figure 3 shows plots of the integrated kinetic energy (exact, TF functional, and pure TF) as a function of the scaled magnetic field strength, ω (recall from the definition that $\omega = 0$ corresponds to no magnetic field, and $\omega \to 1$ corresponds to the field going to infinity). As seen from the graphs, the TF functional does not produce the exact kinetic energy at finite magnetic field strengths, but nonetheless closely follows the exact kinetic energy, particularly at weak field strengths. The kinetic energy has a pronounced step-like form, with discrete jumps occurring at certain values of ω as the magnetic field is increased. Again, the pure TF expression is a smooth curve that follows the general trend of the exact energy. As expected, the TF functional becomes more accurate as the number of particles is increased. For example, figure 3(*b*) compares the integrated kinetic energy densities for $\mathcal{N} = 210$ particles; the exact and TF curves are nearly indistinguishable,

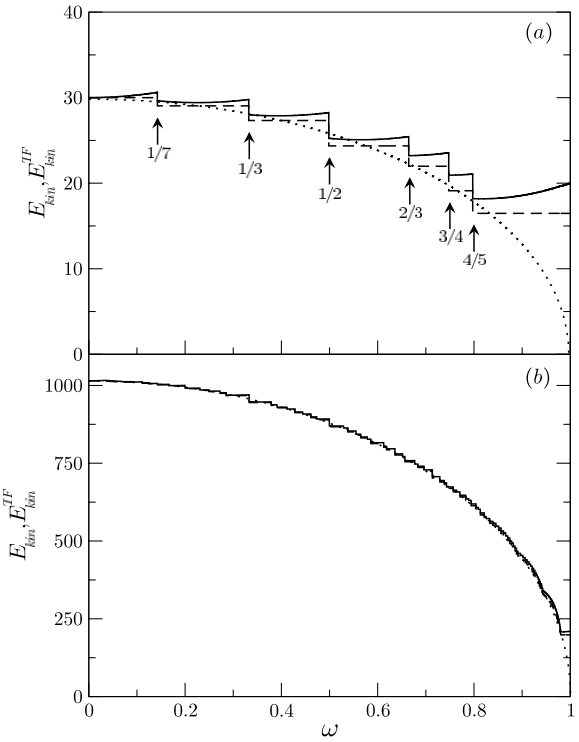

Figure 3. $T = 0$ integrated kinetic energy, plotted against the scaled magnetic field strength, ω. Panel (a) is for $\mathcal{N} = 20$ particles, and panel (b) is for $\mathcal{N} = 210$. The arrows in panel (a) indicate the special values of ω for which a discontinuity in the integrated kinetic energy occurs. These arrows correspond to the special values of ω, indicated by solid circles, in figure 4.

except when the field becomes very strong. Notice, however, that the pure TF calculation (dotted line) becomes increasingly inaccurate as $\omega \to 1$; it incorrectly approaches zero (in units of $\hbar\omega_{\text{eff}}$),[2] whereas the exact energy approaches $E_{\text{kin}} = \mathcal{N}$, which is expected if all of the particles are in the lowest Landau level.

3. Quantum mechanical effects

We will now examine the origin of the steps that occur in the integrated kinetic energy (see figure 3) as the strength of the magnetic field is varied. With [4, 5] in mind, we will also subsequently examine the step-like features exhibited by the chemical potential as the particle number is varied, for both the zero and finite-magnetic field cases.

3.1. Kinetic energy

Figure 4 shows a plot of the single particle energy levels (i.e., Fock–Darwin spectrum) of the system as a function of the scaled magnetic field strength ω. As the magnetic field strength is changed, the order of the energy levels from lowest to highest energy changes as they cross

[2] As the magnetic field is increased, the TF kinetic energy stays constant, at $E^{\text{TF}} = \frac{1}{3}\hbar\omega_o\mathcal{N}^{3/2}$. However, since $\omega_{\text{eff}} \to \infty$ as the magnetic field gets large, $\frac{E^{\text{TF}}}{\hbar\omega_{\text{eff}}} \to 0$.

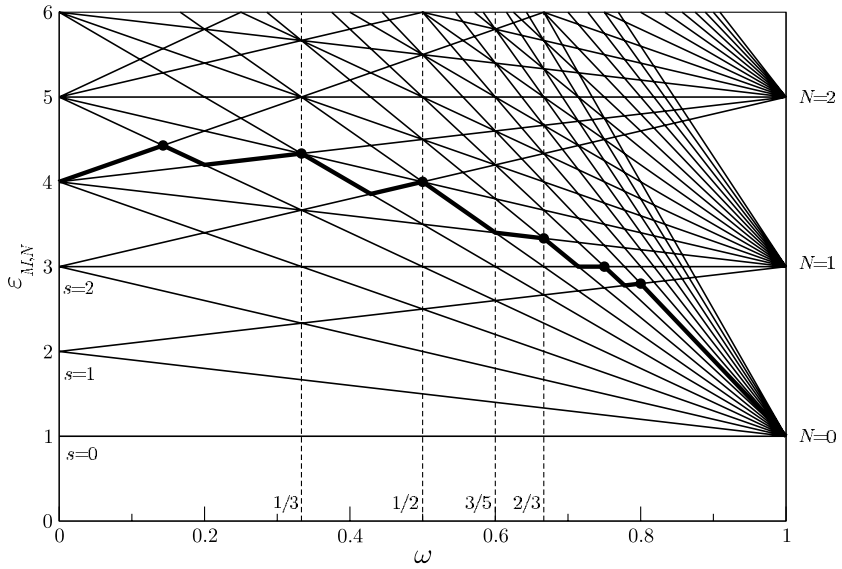

Figure 4. Energy level spectrum for harmonically confined particles is a magnetic field. The left side (at $\omega = 0$) corresponds to the degenerate shells of an isotropic harmonic oscillator, while the right side (at $\omega = 1$) corresponds to the Landau levels of a uniform gas in a magnetic field. The bold line traces the Fermi energy for $\mathcal{N} = 20$ particles, while the solid circles give the values of ω where the steps occur in the kinetic energy. The dashed lines indicate the special values of ω as discussed in section 3.2. For clarity, only states originating from the first 15 harmonic oscillator shells are shown.

on the diagram. At low temperatures, therefore, the highest energy particles will move into different states as the field strength is changed in order to ensure that only the lowest energy states are occupied. It is at these values of ω, for which a previously unoccupied state becomes occupied, that the steps in the kinetic energy occur.

To illustrate this, the bold line in figure 4 traces the Fermi energy for $\mathcal{N} = 20$ particles. The values of ω corresponding to the steps in the kinetic energy are marked by solid circles. The location of the solid circles in this figure correspond to the arrows shown in figure 3(*a*).

3.2. Chemical potential

In the work of Schneider and Toms [4, 5], it was found that the (zero magnetic field) chemical potential as a function of the number of particles displays discrete steps at particle numbers determined by the filling of the harmonic oscillator shells, which gradually smooth out as the temperature is increased. Figures 5 and 6 show the chemical potential at various temperatures for $\omega = 0$, and $\omega = 0.5$, respectively. Also included is the pure TF approximation to the chemical potential (again given by the dotted line).

At finite magnetic field strengths, the chemical potential shows a similar structure to the zero field case (i.e., figure 5), except that the particle numbers at which the steps occur, the so-called 'magic numbers' in the language of [4], depends on the value of ω. As was observed in [4, 5] for the special case of $\omega = 0$, as T increases the steps in the chemical potential begin to smooth out. This results in the TF expression becoming more accurate, thereby confirming that the origin of these steps is purely quantum mechanical (i.e., the discrete energy level structure of the system).

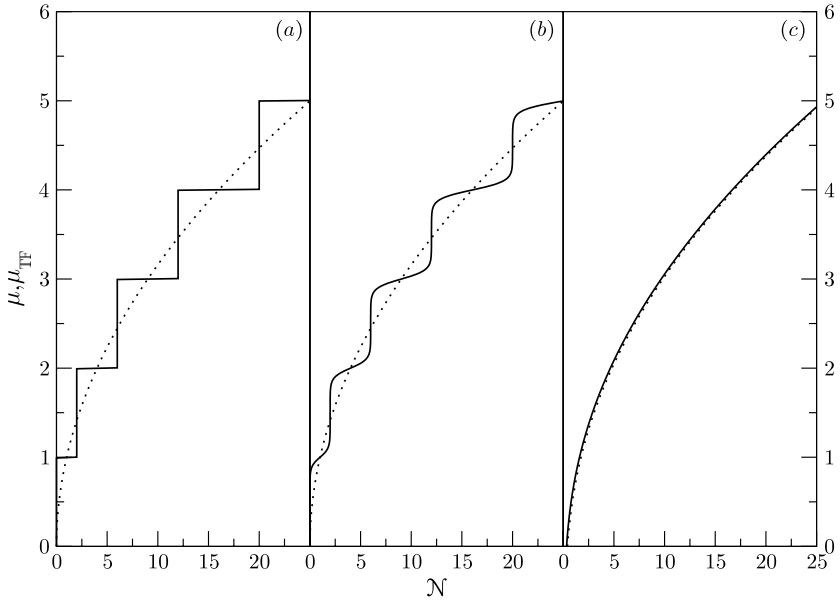

Figure 5. Chemical Potential as a function of particle number at $\omega = 0$. Panel (a) is for $T = 0$, panel (b) is for $T = 0.05$, and panel (c) is for $T = 0.5$.

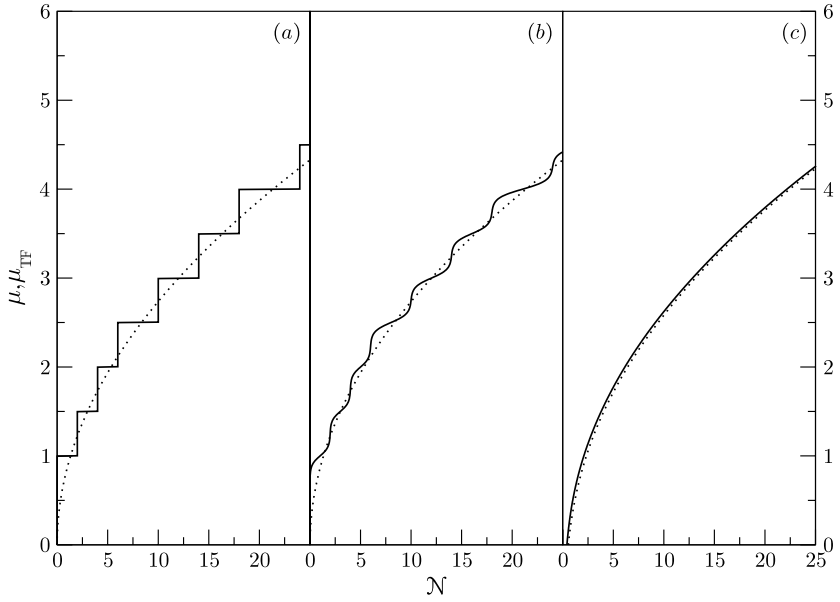

Figure 6. Same as figure 5, but for $\omega = 0.5$.

At zero temperature, the chemical potential equals the Fermi energy, the energy of the highest occupied level. As the number of particles is increased, the Fermi energy will not change until all degenerate states with the same energy are filled, and the next highest energy level must be occupied. The values of the 'magic numbers' at which the steps occur are

therefore determined by the degeneracy of the energy levels. We will now examine how the degeneracy of the levels depends on the magnetic field strength, with a view to explaining the steps seen in figures 5 and 6.

The energy levels, equation (8), may be written as

$$\epsilon_{MN} = 1 + (1-\omega)M + (1+\omega)N. \tag{27}$$

While it is difficult to analyse the degeneracy of these levels for arbitrary ω, we can nonetheless get some understanding of the steps in the chemical potential by considering the following special case. Equation (27) will have the simplest mathematical structure when $(1+\omega) = i(1-\omega)$, where i is an integer, since in that case the levels will all be evenly spaced. This assumption implies that

$$\omega = \frac{i-1}{i+1}. \tag{28}$$

Thus, when equation (28) is satisfied, the energy levels will be

$$\epsilon_k = 1 + (1-\omega)k, \qquad k = 0, 1, 2 \ldots. \tag{29}$$

and the degeneracy will be given by

$$\nu_k = \left\lfloor \frac{k}{i} \right\rfloor + 1 = \left\lfloor \left(\frac{1-\omega}{1+\omega} \right) k \right\rfloor + 1. \tag{30}$$

The energy levels thus have, in this simple case, a form analogous to an isotropic harmonic oscillator, with evenly spaced increasingly degenerate levels. The degeneracy, however, only increases with every i levels, rather than with every level. For example, $\omega = \frac{1}{3}$ gives $i = 2$, and $\nu_k = \lfloor \frac{k}{2} \rfloor + 1$, so that the degeneracy increases with every second energy level. The first few of these special values of ω are highlighted in figure 4 by dashed lines (note that these values *do not* necessarily correspond to steps in the kinetic energy).

The Fermi energy is related to the particle number by

$$\mathcal{N} = 2 \sum_{k=0}^{k_f} \nu_k. \tag{31}$$

Making use of (30), a careful evaluation of the sum yields

$$\mathcal{N} = \left(2k_f - \mathrm{i} \left\lfloor \frac{k_f}{i} \right\rfloor \right) \left\lfloor \frac{k_f}{i} \right\rfloor + (2-i) \left\lfloor \frac{k_f}{i} \right\rfloor + 2k_f + 2. \tag{32}$$

Equation (32) will give the 'magic numbers' at which the steps in the chemical potential occur (at $T = 0$), when ω satisfies condition (28).

For the special case of $i = 1$ ($\omega = 0$), equation (32) reduces to the correct expression for the number of particles in $k_f + 1 = \mathcal{M} + 1$ filled shells of an isotropic harmonic oscillator, namely $\mathcal{N} = \mathcal{M}^2 + 3\mathcal{M} + 2$, as given in [3]. This will require that $\mathcal{N} \in \{2, 6, 12, 20, 30, \ldots\}$, which can be directly verified from figure 5. Taking $i = 3$, so that $\omega = 1/2$, as in figure 6, gives $\mathcal{N} \in \{2, 4, 6, 10, 14, \ldots\}$. It also follows that if ω is irrational there will be no degenerate energy levels, and steps will therefore occur at every second particle number (or every particle number if the spin degeneracy factor is omitted). This explanation for the origin of the steps is, in our opinion, more intuitive than the one presented by Toms, which was based on a decomposition of the thermodynamic potential into a sum of a smooth and oscillatory terms with the oscillatory part interpreted in analogy of the de Haas-van Alphen effect. Our analysis makes it quite clear what the physical origin of these steps are, and is valid for zero or finite magnetic fields.

4. Limiting cases

We will now consider several limiting cases, obtaining simplified analytical expressions. The first case we will consider is the limit of large particle numbers, where we will show analytically that, at zero temperature, the exact expressions for both the chemical potential and the kinetic energy approach the pure TF values when $\mathcal{N}$ becomes large. We will also consider the limits of both strong and weak magnetic fields, where we derive simplified expressions for the kinetic energy and chemical potential (again at zero temperature), and obtain conditions on the magnetic field strength for the expressions to be valid.

4.1. Large $\mathcal{N}$ limit

We first consider the Fermi energy, which is related to the particle number by

$$\mathcal{N} = 2\sum_{M,N}\Theta(\epsilon_f - \epsilon_{MN}) \tag{33}$$

$$= 2\sum_{N=0}^{\lfloor\frac{\epsilon_f-1}{1+\omega}\rfloor}\left(\left\lfloor\frac{\epsilon_f - 1 - (1+\omega)N}{1-\omega}\right\rfloor + 1\right) \tag{34}$$

$$= 2\sum_{N=0}^{\lfloor\frac{\epsilon_f-1}{1+\omega}\rfloor}\left(\frac{\epsilon_f - 1 - (1+\omega)N}{1-\omega} + 1\right) - 2\sum_{N=0}^{\lfloor\frac{\epsilon_f-1}{1+\omega}\rfloor}\left\{\frac{\epsilon_f - 1 - (1+\omega)N}{1-\omega}\right\}, \tag{35}$$

where $\{x\}$ denotes the fractional part of x, i.e. $x = \lfloor x\rfloor + \{x\}$. In the limit as $\mathcal{N}$ becomes large, ϵ_f also becomes large, and so the floor function in the limits of the sums in equation (35) will be well approximated by the argument. Similarly, the second sum in equation (35) becomes negligible; an upper bound on this sum is $2\left(\frac{\epsilon_f-1}{1+\omega}+1\right)$. Evaluating the remaining sum in (35) then leads to

$$\mathcal{N} = \frac{\epsilon_f^2 + (1-\omega)\epsilon_f + \omega - 2\omega^2}{1-\omega^2}, \tag{36}$$

which will be valid provided that

$$2\left(\frac{\epsilon_f - 1}{1+\omega} + 1\right) \ll \frac{\epsilon_f^2 + (1-\omega)\epsilon_f + \omega - 2\omega^2}{1-\omega^2}, \tag{37}$$

which implies

$$\epsilon_f \gg 1. \tag{38}$$

In the limit as ϵ_f becomes large, the quadratic term will dominate, giving $\epsilon_f = \sqrt{(1-\omega^2)\mathcal{N}}$, which is exactly the pure TF result, namely,

$$\mathcal{N} = \frac{1}{\pi}\int_0^{\sqrt{2\epsilon_f/(1-\omega^2)}} \rho_{\mathrm{TF}}(\vec{r})d\vec{r}$$
$$= \frac{\epsilon_f^2}{1-\omega^2}.$$

It also readily shown that starting from equation (25), the exact kinetic energy also approaches the pure TF value of $E_{\mathrm{kin}}^{\mathrm{TF}} = \frac{1}{3}\sqrt{1-\omega^2}\mathcal{N}^{3/2}$ (i.e., obtained from integrating equation (19) with equation (20) inserted). As mentioned above, however, the TF expressions will become less and less accurate as $\omega \to 1$, for a *fixed* number of particles. In this case, the appropriate limit for correctly reducing to the pure TF result is $\mathcal{N} \to \infty$ as $\omega \to 1$.

4.2. Strong fields

It can be seen from figure 4 that for strong magnetic fields, which correspond to $\omega \to 1$, all particles will, at zero temperature, be in an $N = 0$ state. In this limit the energy of the occupied levels will be given by

$$\epsilon_M = 1 + (1 - \omega)M, \tag{39}$$

with the highest allowed value of M corresponding to $\mathcal{N} = 2(M_f + 1)$. As can be seen from figure 4, the boundary to this strong field regime is defined by the value of ω for which the highest occupied $N = 0$ level intersects with the lowest energy $N = 1$ level on the diagram. Thus the magnetic field strengths for which the following expressions will be valid are defined by

$$1 + (1 - \omega)M_f \leqslant 1 + (1 + \omega), \tag{40}$$

which gives

$$\omega \geqslant \frac{M_f - 1}{M_f + 1} = \frac{\mathcal{N} - 4}{\mathcal{N}}. \tag{41}$$

The condition on ω above will be satisfied for large magnetic fields and low numbers of particles. For example, $\mathcal{N} = 20$ particles will require that $\omega \geqslant 0.8$ (see figures 3 and 4).

The chemical potential, which at zero temperature is the Fermi energy, is given by

$$\epsilon_f = \omega + \frac{1 - \omega}{2}\mathcal{N}. \tag{42}$$

Note that unlike equation (36), there are no quadratic terms in ϵ_f. Therefore, when equation (41) is satisfied, the Fermi energy and particle number are related by a simple linear relationship. The integrated kinetic energy can also be calculated from equation (25) as

$$E_{\text{kin}} = \tfrac{1}{2}(1 - \omega)^2 M_f^2 + \left(\tfrac{3}{2}\omega^2 - \omega + \tfrac{3}{2}\right) M_f + 1 + \omega^2. \tag{43}$$

The density matrix may also be easily simplified in the present limit by making use of the form given in equation (2). Identifying $N = n + l$, as discussed above, we set $n = l = 0$ in equation (2) to obtain the simple expression:

$$\begin{aligned}\rho(\vec{r}, \vec{r}_0) &= \frac{2}{\pi}\sum_{m=0}^{M_f} L_0^m(2\mathcal{A})\frac{\mathcal{B}^m}{m!}\,\mathrm{e}^{-\mathcal{A}} = \frac{2}{\pi}\,\mathrm{e}^{-\mathcal{A}}\sum_{m=0}^{M_f}\frac{\mathcal{B}^m}{m!} \\ &= \frac{2}{\pi}\frac{\mathrm{e}^{\mathcal{B}-\mathcal{A}}}{M_f!}\Gamma(M_f + 1, \mathcal{B}).\end{aligned} \tag{44}$$

To our knowledge the above expression has not previously appeared in the literature, and may prove useful in further analytical studies of low temperature Fermi gases.

4.3. Weak fields

In the limit of weak magnetic fields it is more natural to write the energy levels as

$$\epsilon_{sl_z} = 1 + s + \omega l_z \qquad s = 0, 1, 2, \ldots \qquad l_z = -s, -s + 2, \ldots, \tag{45}$$

where s is the index of the harmonic oscillator shell, and l_z is the angular momentum (in the z-direction), and obviously $s = M + N$, $l_z = N - M$. The weak magnetic field limit is defined by the region before the first step in the kinetic energy, or referring to figure 4, the region to the left of where the energy levels first cross. In this region, the shells of the isotropic harmonic oscillator will be filled successively, with the degenerate levels in each shell, corresponding

to particles with different angular momenta, being split by the magnetic field. For simplicity, we will assume completely filled oscillator shells. Assuming $\mathcal{M}+1$ filled shells, this region is defined by

$$1+\mathcal{M}+\omega\mathcal{M} \leqslant 1+(\mathcal{M}+1)+\omega(-\mathcal{M}-1), \tag{46}$$

which gives

$$\omega \leqslant \frac{1}{2\mathcal{M}+1}. \tag{47}$$

The condition on ω above will be satisfied for low magnetic fields. Again, referring to figures 3 and 4, $\mathcal{N}=20$ particles will require that $\omega \leqslant \frac{1}{7}$. Also, note that the number of filled shells is related to the number of particles by $\mathcal{N}=\mathcal{M}^2+3\mathcal{M}+2$, as was mentioned in the previous section.

Focusing on the same quantities as in the high field limit, we find the Fermi energy to be

$$\epsilon_f = 1+(1+\omega)\mathcal{M}, \tag{48}$$

which reduces to the correct value for the Fermi energy in the absence of a magnetic field, $\epsilon_f = 1+\mathcal{M}$, as given in [3, 10]. The total kinetic energy may be calculated from equation (25) as

$$\begin{aligned} E_{\text{kin}} &= (1+\omega^2)\left(\tfrac{1}{3}\mathcal{M}^3+\tfrac{3}{2}\mathcal{M}^2+\tfrac{13}{6}\mathcal{M}+1\right) \\ &= (1+\omega^2)E_{\text{kin}}^{(0)}, \end{aligned} \tag{49}$$

where $E_{\text{kin}}^{(0)}$ is the expression for the exact kinetic energy at $\omega=0$ [3] (but scaled here by the effective frequency, $\hbar\omega_{\text{eff}}$, rather than $\hbar\omega_o$).

Since all of the same states are occupied as in the $\omega=0$ case, and the wavefunctions, namely, equation (7), do not depend explicitly on ω, the density matrix will be identical in a form to that for a system of fermions in an isotropic harmonic oscillator with no external magnetic field, as given in [2, 3], the only change being in the scaling of the variables. This is further evidenced by the fact that the TF kinetic energy (which depends on the diagonal part of the density matrix) is constant in this region (see figure 3), and indeed only changes in discrete steps. In the low field regime, therefore, the TF kinetic energy is simply

$$E_{\text{kin}}^{\text{TF}} = E_{\text{kin}}^{(0)}. \tag{50}$$

Upon comparing equations (49) and (50), it can be seen that the TF functional only gives the *exact* integrated kinetic energy when $\omega=0$, although it will be very close for small ω. This analytical result is an affirmation of the surprising finding in [3], in which it was shown that the TF functional (with the exact density as input and no gradient corrections) integrates to the exact quantum mechanical kinetic energy at zero magnetic field. We have now shown, however, that in the presence of an external magnetic field, this result is no longer true.

We emphasize that the expressions given in this and the previous section are not asymptotic limits, but are exact under the given restrictions; referring to figure 3, they correspond to the first and last steps in the diagram.

5. Conclusions

We have presented an analytical study of an ideal charged quantum gas confined by a harmonic potential in two dimensions. While we have focused our attention to the case of fermions, our exact expressions for the density matrix and kinetic energy density can be easily applied to bosons, the only change being the '+1' in the denominator of equation (4) replaced by a '−1' (in addition to dropping the spin degeneracy of two in the case of spinless bosons).

Unlike other studies of this kind, our results include a constant magnetic field of arbitrary magnitude in the perpendicular direction and are valid at any finite temperature, though we have restricted our attention primarily to $T = 0$. We have focused on a comparison of the exact quantities with those obtained from the TFA, and motivated by the findings of [3], have shown analytically that the 2D TF kinetic energy density functional *does not* integrate to the exact quantum mechanical kinetic energy when a magnetic field is introduced. The TF functional does, however, still do surprisingly well at reproducing the quantum mechanical oscillations in the kinetic energy density, even at low numbers of particles (i.e., $\mathcal{O}(10^2)$), where it is not necessarily expected to be accurate, particulary in the absence of gradient corrections.

We have also provided, in our opinion, a much simpler interpretation for the origin of the step-like structures exhibited by the integrated kinetic energy and chemical potential (at zero and finite magnetic fields) which were first noted in [4, 5] for the chemical potential at zero magnetic field. We have also shown analytically that in the limit $\mathcal{N} \to \infty$, the exact expressions for the kinetic energy, and the Fermi energy approach those found in the TF theory, in addition to providing some simplified expressions of our exact results valid for high and low magnetic field strengths.

Acknowledgments

This research was supported through a grant from the National Research and Engineering Council of Canada (NSERC).

References

[1] Shea P and van Zyl B P 2006 *Phys. Rev.* B **74** 205334
[2] Shea P and van Zyl B P 2007 *J. Phys. A: Math. Theor.* **40** 10589
[3] Brack M and van Zyl B P 2001 *Phys. Rev. Lett.* **86** 1574
[4] Schneider J and Wallis H 1998 *Phys. Rev.* A **57** 1253
[5] Toms D J 2005 *Ann. Phys.* **320** 487
[6] Gradshteyn I S and Ryzhik I M 1980 *Table of Integrals, Series and Products* 4th edn ed A Jeffrey (New York: Academic)
[7] van Zyl B P and Hutchinson D A W 2004 *Phys. Rev.* B **69** 024520
[8] Brack M and Bhaduri R K 1997 *Semiclassical Physics (Frontiers in Physics* vol 96) (Reading, MA: Addison-Wesley)
[9] Ghosh S K and Dhara A K 1990 *Phys. Rev.* A **40** 6103
[10] Brack M and Murthy M V N 2003 *J. Phys. A: Math. Gen.* **36** 1111
[11] Bhaduri R K, Li S, Tanaka K and Waddington J C 1994 *J. Phys. A: Math. Gen.* **27** L553
[12] Habeeb M A Z 1987 *J. Phys. A: Math. Gen.* **20** 5549